Department of Veterans Affairs

JRRD Volume 45, Number 9, 2008
Pages 1303–1316
Journal of Rehabilitation Research & Development

Effect of inaccuracies in anthropometric data and linked-segment inverse dynamic modeling on kinetics of gait in persons with partial foot amputation

Michael P. Dillon, BPO(Hons), PhD;[1*] Timothy M. Barker, BE(Hons), PhD;[2] Graeme Pettet, PhD[3]
[1]National Centre for Prosthetics and Orthotics, Musculoskeletal Research Centre, Faculty of Health Sciences, La Trobe University, Bundoora, Victoria, Australia; [2]Stryker Pacific, West End, Brisbane, Queensland, Australia; [3]School of Mathematical Sciences, Queensland University of Technology, Brisbane, Queensland, Australia

Abstract—The accuracy of data derived from linked-segment models depends on how well the system has been represented. Previous investigations describing the gait of persons with partial foot amputation did not account for the unique anthropometry of the residuum or the inclusion of a prosthesis and footwear in the model and, as such, are likely to have underestimated the magnitude of the peak joint moments and powers. This investigation determined the effect of inaccuracies in the anthropometric input data on the kinetics of gait. Toward this end, a geometric model was developed and validated to estimate body segment parameters of various intact and partial feet. These data were then incorporated into customized linked-segment models, and the kinetic data were compared with that obtained from conventional models. Results indicate that accurate modeling increased the magnitude of the peak hip and knee joint moments and powers during terminal swing. Conventional inverse dynamic models are sufficiently accurate for research questions relating to stance phase. More accurate models that account for the anthropometry of the residuum, prosthesis, and footwear better reflect the work of the hip extensors and knee flexors to decelerate the limb during terminal swing phase.

Key words: accuracy, amputation, anthropometric, gait, inverse dynamic, kinetics, linked-segment, models, moments, partial foot, rehabilitation.

INTRODUCTION

Linked-segment models of the human body have proven useful in estimating those determinants of human walking that cannot be directly measured, such as joint reaction forces or muscle moments. The process used to derive these parameters is known as inverse dynamics, because one can work back from the kinematic, anthropometric, and externally measured force data to derive the kinetics responsible for the motion.

The accuracy of data derived from the linked-segment model depends on how well the system being studied has been represented and on the assumptions of the model. Other sources of error may be derived from the kinematic, anthropometric, or ground reaction force data used by the model and include, for example, estimation of joint rotation centers [1–2], movement of markers on the skin [3], variation in segment lengths [4], estimation of body segment parameters [5–6], variation in cadence and

Abbreviations: BSP = body segment parameters, CM = center of mass, CV = center of volume, I = mass moment of inertia, PFA = partial foot amputation, PTB = patellar tendon-bearing.

***Address all correspondence to Michael P. Dillon, BPO(Hons), PhD; National Centre for Prosthetics and Orthotics, La Trobe University, Bundoora 3086, Australia; +61-3-9479-5889; fax: +61-3-9479-5784. Email: Michael.Dillon@latrobe.edu.au**

DOI:10.1682/JRRD.2007.11.0190

stride length [7], and errors in measurement of the magnitude and position of the ground reaction force [6].

Analysis of the gait of persons with amputation may violate some of the basic assumptions of a conventional linked-segment model (e.g., the freely articulating anatomical ankle has been replaced by a solid ankle foot) or may require customized anthropometric data to accurately describe the system (e.g., a portion of the anatomical leg has been replaced by a titanium pylon).

Previous studies on persons with transfemoral and transtibial amputation have attempted to address these issues by estimating anthropometric characteristics of the prosthesis [8–11] and residual limb [8,12–13] to provide more accurate anthropometric input data. Previous studies on persons with partial foot amputation (PFA) have not addressed either of these issues [14–17].

Most investigators of the gait of persons with PFA have focused on individuals with relatively distal amputation(s) in conditions of barefoot walking [15–16] and orthotic intervention [14,17]. As such, consideration of more accurate anthropometric input data may have seemed unnecessary, given that small changes in anthropometric input data are believed to have little impact on the accuracy of muscle moment data in people without amputation [6]. However, when amputation affects significant portions of the forefoot (e.g., Chopart and Lisfranc amputation) and prosthetic intervention is more extensive (e.g., clamshell device), the validity of this assumption seems less robust. To elaborate, not just the anthropometry of the residuum is considerably altered. Once the metatarsals are affected, atrophy of the triceps surae is observable, indicating a likely reduction in the mass and mass moment of inertia (*I*) of the leg segment. Moreover, the clamshell prostheses that are commonly fitted at these proximal amputation levels are quite heavy and the socket encompasses the residual foot and leg segment, thus eliminating ankle motion. The device also has a center of mass (CM) somewhere near the ankle, and as such, the value of *I* is expected to be considerable.

Given an appreciation of the linked-segment models used in previous investigations [14–17] and their inaccuracies in modeling the anthropometry of the partial foot residuum and prosthetic replacement, one may glean some indication of the errors that could be expected in the kinetic data.

During swing phase, the joint moments are expected to be most affected by errors in the anthropometric input data. During swing phase, the moment equations are more sensitive to changes in the mass and *I* terms because of the absence of the large external forces and joint compressive forces that dominate the moment equations during stance. Moreover, swing phase creates large accelerations that compound the effect of the anthropometric changes. Changes are expected to be observed at the hip and knee joints, where the respective segment masses are large and accelerations are greatest. Obviously, changes in the joint moments will also be reflected in measures of power generation/absorption, given that power is the product of the moment and angular velocity.

The requirement for a customized linked-segment inverse dynamic model seems self-evident given that the unique anthropometry of the affected limb, prosthesis, and footwear has not been well modeled. Customizing a linked-segment model to investigate the effect of more accurate modeling on the kinetics of gait would require customized anthropometric input data describing the residuum, proximal limb segments (e.g., the leg to account for atrophy of the triceps surae), prosthesis, and footwear. While the physical characteristics of the prosthesis and footwear could be easily obtained by standard dynamics techniques [18], the same anthropometric descriptions of the residuum are not so easily obtained.

Numerous methods exist for determining these body segment parameters (BSP) data. The most common approaches include proportional data sets, incremental immersion, and geometric models.

Proportional anthropometric data sets estimate BSP by using regression equations, typically based on cadaver studies, whereby segment characteristics are determined as a proportion of body mass and stature. Given that PFA does not alter stature or significantly alter total body mass, despite significantly changing the foot segment, the sensitivity of this approach seems limited.

Incremental immersion is a convenient and inexpensive method of measuring volume and center of volume (CV), but it is time consuming. If an assumption is made about density, then mass and CM can also be determined. This technique has been used with good results on nondisabled subjects [19–20] and subjects with transtibial [21] and transfemoral amputation [12]. Some authors have measured volume of a prosthetic socket [8] or plaster cast of the residuum [12] as alternatives; the latter also allows the measurements of *I* or the radius of gyration to be calculated with “torsional table” or “pendulum” methods [22–24]. Using replicas of limb segments also overcomes the difficulties of executing the measurements reliably, accurately, and in a timely fashion on living subjects.

Geometric models determine BSP by using an assemblage of geometric shapes to model the limb. These geometric shapes can be described mathematically from a few simple measurements, such as the segment length and circumferences [25–26]. This approach has the advantage that it can, in principle, be applied to any population [2], although the resulting accuracy is often not adequately reported [25–26]. While these models can be time-consuming to develop, once complete they provide a convenient way to estimate these BSP.

In summary, the requirement that methods easily and accurately estimate anthropometric input data of the residuum, prosthesis, and footwear and incorporate these input data into customized linked-segment inverse dynamic models is a necessary step toward understanding the degree to which errors in these anthropometric input data influence the kinetics of gait. Future investigators should be better informed about the rigorousness of the anthropometric input data required, particularly given that research on persons with PFA has increased over the last decade [27] because in some parts of the world the incidence of PFA eclipses that of transtibial and transfemoral amputations combined [28].

The aims of this investigation were to—

1. Develop a geometric model to estimate the mass, CM, and *I* of intact and partial feet.
2. Determine the strength of the linear relationship between modeled and experimentally derived BSP data obtained by using incremental immersion and torsional table measurements of plaster replicas of intact and partial feet.
3. Develop a customized linked-segment inverse dynamics model that accounts for the unique anthropometry of the partially amputated foot, altered proximal limb segments, prosthesis or orthosis, and footwear.
4. Describe the changes in anthropometry of the modeled limb segments when using the customized and conventional linked-segment model.
5. Compare the peak joint moments and powers derived with the customized and conventional linked-segment models.

We hypothesized that a strong and significant relationship would exist between modeled and experimentally derived BSP data, thus demonstrating the reasonableness of the modeled estimates in relation to previously well-accepted experimental techniques. We also hypothesized that, as compared with the conventional model, the customized linked-segment model would significantly increase the peak moments and powers during swing phase at both the hip and knee joints and that changes to the stance phase kinetics would be modest.

METHODS

Subjects

Subjects with amputation were identified through either the Queensland Amputee Limb Service or prosthetic service providers in Queensland, Australia. Subjects were excluded if they ambulated with the use of any gait aids or had concomitant health problems such as ulceration or neuromuscular/musculoskeletal conditions that might affect their gait. Children were excluded because of the lengthy testing sessions. Diabetes or peripheral vascular disease were not considered criteria for exclusion. Of the 56 individuals invited through these avenues, 14 responses were received. Six of these fourteen respondents met the exclusion criteria, and as such, data were collected on only eight individuals. Nine persons without limb loss were recruited through convenience sampling within the university and matched for sex, age, and mass to one of the participants with amputation (for a concurrent investigation). Individuals without limb loss satisfied the same exclusion criteria as the persons with PFA. Participants provided informed consent as required by the University Human Research Ethics Committee of the Queensland University of Technology.

To examine the reasonableness of the geometric model, we collected data on the residua of all 8 persons with PFA, including 2 persons with bilateral amputation; this resulted in data on 10 residua, including 2 metatarsophalangeal, 1 transmetatarsal, 5 Lisfranc, and 2 Chopart. We also collected BSP on the persons without limb loss to evaluate the reasonableness of the model for estimating BSP for the intact foot. Anthropometric characteristics of the subject groups have been reported in **Table 1**.

To compare kinetic data generated using the customized and conventional linked-segment models, we used a subset of the PFA subjects with unilateral amputation (**Table 2**). In this way, BSP data from the sound limb could be used as input data into the conventional linked-segment model. Four subjects in this subsample wore either toe-fillers or slipper sockets and were assigned to Sample A because these devices allowed unrestricted ankle motion, which necessitated a particular approach to

Table 1.
Anthropometric characteristics of all subjects with and without amputation. Mean ± standard deviation (SD) for stature, body mass, residual foot length (RFL), and intact foot length (IFL) are presented. SD values for stature and mass were not reported for subjects with metatarsophalangeal (MTP) and transmetatarsal (TMT) amputations because each group only had one subject. Subject with MTP amputation had bilateral amputations of the same length; hence, SD values are reported for RFL. IFL data were estimated for bilateral partial foot amputation based on regression equations linking stature and IFL [1]. Eight subjects had amputation, two of whom had bilateral amputation. Hence, the total sample included 10 residua.

Anthropometric Characteristic	Nondisabled (*n* = 9)	Amputation (*n* = 10)	Amputation Subsample			
			MTP (*n* = 2)	TMT (*n* = 1)	Lisfranc (*n* = 5)	Chopart (*n* = 2)
Stature (m)	1.81 ± 0.07	1.75 ± 0.08	1.74	1.82	1.74 ± 0.11	1.77 ± 0.02
Body Mass (kg)	85.49 ± 9.20	73.10 ± 14.95	64.85	84.50	67.74 ± 16.30	89.05 ± 5.59
Foot Length						
IFL (m)	0.27 ± 0.01	0.26 ± 0.01	0.26 ± 0.00	0.27	0.26 ± 0.01	0.27 ± 0.01
RFL (m)	—	0.15 ± 0.03	0.20 ± 0.00	0.17	0.14 ± 0.02	0.11 ± 0.00
RFL (%IFL)	—	52.67 ± 12.64	76.72 ± 0.54	62.26	55.36 ± 5.42	41.15 ± 1.63

1. Dempster WT. Space requirements of the seated operator: Geometrical, kinematic, and mechanical aspects of the body, with special reference to the limbs. Technical Report WADC-TR-55-159. Wright-Patterson Air Force Base (OH): Aerospace Medical Research Laboratory; 1955.

Table 2.
Characteristics of subjects with amputation in linked-segment modeling portion of study.

Subject	Amputation Level	Etiology	Age (yr)	Stature (m)	Mass (kg)	Type of Fitting
Sample A: With Ankle Motion						
2103-2116A	TMT	Trauma	54	1.82	84.5	EVA toe-filler with casual leather walking shoes.
2103-1906A	Lisfranc	Trauma	55	1.80	80.7	Sock stuffed in running shoe.
2703-1903A	Lisfranc	Trauma	53	1.82	76.6	Running shoe with acrylic resin below ankle slipper socket with silicone liner. Foam forefoot bonded onto socket and covered with leather.
0704-0403A	Lisfranc	Trauma	22	1.84	81.5	Running shoe with carbon fiber below ankle slipper socket. EVA forefoot covered in leather.
Mean ± SD			46 ± 16	1.82 ± 0.02	80.8 ± 2.8	—
Sample B: Without Ankle Motion						
3004-1102A	Chopart	Trauma	19	1.79	93.0	Running shoe with acrylic laminated clamshell socket with SACH foot bonded onto inferior and anterior aspect of socket.

EVA = ethylene vinyl acetate, SACH = solid-ankle cushioned heel, SD = standard deviation, TMT = transmetatarsal.

development of the linked-segment model. The remaining subject had a Chopart amputation and presented wearing a clamshell patellar tendon-bearing (PTB) prosthesis; this subject was the only one in Sample B because this device eliminated ankle motion, which necessitated a different approach to development of the linked-segment model.

Apparatus

Geometric Model of Foot

Dimensional and inertial characteristics of the partial and intact feet were derived with a geometric model based on work by Hatze [25]. The model was coded in MATLAB 5.3 (MathWorks Inc; Natick, Massachusetts) and is available online through the Australasian Digital Theses Program [29]. The model contained an assemblage of trapezoidal and parabolic plates (**Figure 1**). The mass, CM, and I of each plate comprising the foot was determined with standard equations for those geometric forms. For example, the mass of a trapezoidal plate can be given by the **Equation**

$$m = \frac{\gamma lh(b+c)}{2} \quad ,$$

where γ describes the density of the shape in kilograms per cubic meter, l describes the length of the plate in meters, h describes the thickness or height of the plate in meters, and b and c describe the end widths of the trapezoid in meters (**Figure 1**).

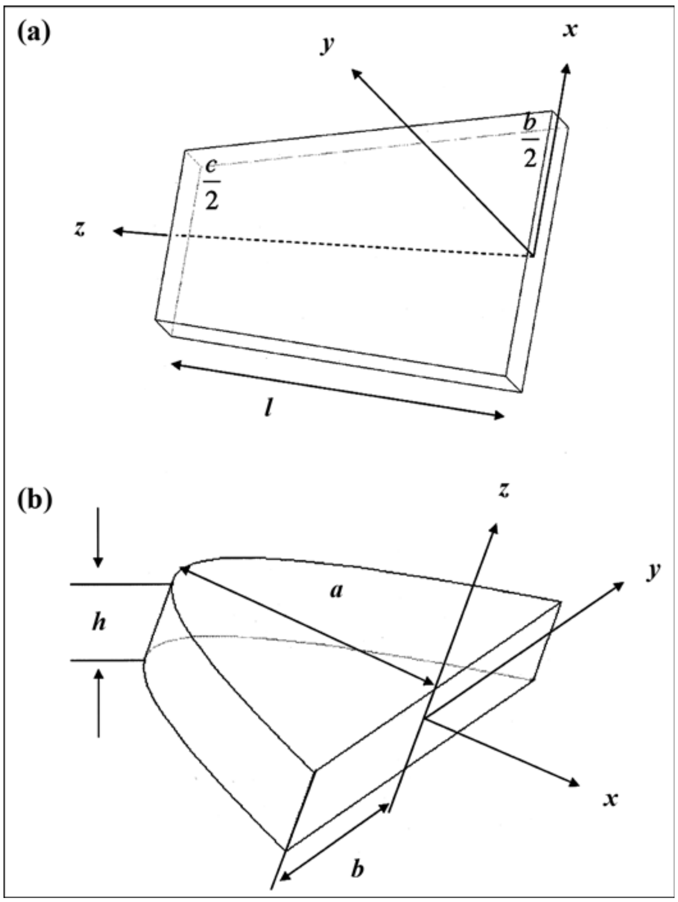

Figure 1.
Basic **(a)** trapezoidal and **(b)** parabolic plates used in construction of geometric model of intact and partial feet. a = length of parabolic plate; b and c = end widths, with b/2 and c/2 = half end widths (to z-axis); h = thickness; l = length of trapezoidal plate.

The total mass of the foot was determined by summing the mass of each component plate of the foot. The same process was used to describe the CM and I of the modeled foot. Given that the computational detail is lengthy, these details have been described elsewhere [30].

A series of trapezoidal plates was used to represent the inferior portion of the ball of the foot (S_{11}), the heel (S_{12}), and the sole above these regions (S_{13}), as depicted in **Figure 2**. The remaining plates accounted for the middle and upper portions of the foot and were described using a combination of trapezoidal (S_{14T}) and parabolic plates (S_{14P}), respectively. The model attempted to describe the equinus deformity often observed in persons with Lisfranc and Chopart residua by varying the height of the longitudinal arch of the foot as a proportion of residual foot length [30]. The model was symmetrical about the x-axis to reduce complexity, as in similar works [25].

To describe the geometric form, the model used 12 input measurements, including residual foot length, lateral malleolus height, and width across the distal end of the remnant foot. A complete set of anthropometric measurements and their exact descriptions have been described in detail elsewhere [30]. Anthropometric calipers and a 30 cm ruler were used to obtain these measurements.

The model has the potential to incorporate varying segment densities that increase from proximal to distal [8] as the proportion of muscle and bone changes [31].

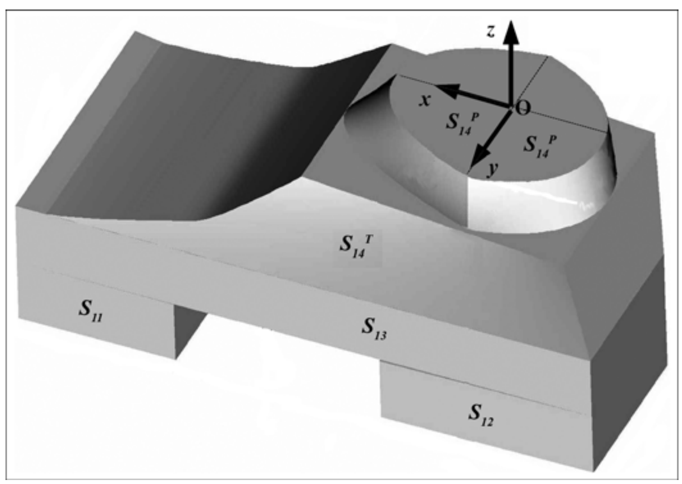

Figure 2.
Geometric model of a metatarsophalangeal residuum. Three trapezoidal plates represent inferior portion of ball of foot (S_{11}), heel (S_{12}), and sole above these regions (S_{13}). Remaining trapezoidal plates account for middle part of foot (S_{14T}). Upper part of foot (S_{14P}) was described with separate parabolic plates.

The segment density values were based on work by Hatze [25] and, on average, were reduced by 9 percent because of the different shape of the proximal portion of the foot model, where the largest segment densities occurred. The derivation of the density assumption has been described in detail elsewhere [30], because it was not relevant for comparison with the plaster replicas in this investigation.

For comparison to the plaster foot replicas, density used in the geometric model was made uniform and equal to that of each plaster foot replica. This enabled the modeled mass, CM, and *I* to be compared with the experimentally derived BSP data obtained with the plaster foot replicas. While this comparison does not help validate the density assumption, it demonstrates the reasonableness of the geometric form in relation to plaster replicas, which reflects the extent to which such models can be reasonably validated.

Experimentally Derived Body Segment Parameters Data for Foot

The replicas of the partial and intact feet were obtained with plaster bandage, and the negative molds were filled with dental plaster [30]. A surform and sand-screen were used to clean up obvious anomalies of the mold.

For the incremental immersion, we used a stainless steel tray to catch the displaced water solution. A cake cooling rack was positioned in the stainless steel tray to keep the immersion container out of the displaced water solution. The plaster feet were immersed in one of two containers, depending on the axis being investigated, so that the opening of the container closely matched the size of the foot. The displaced water solution was decanted and weighed on an electronic scale. The water solution was created from a liquid soap mixed through the water at a rate of 0.25 percent to decrease the water surface tension and avoid the creation of a meniscus during immersion of the plaster feet [30]. The accuracy of the immersion technique and experimental setup was determined using standard geometric forms. Estimates of volume were accurate to 3 percent and estimates of CV were accurate to 4 percent compared with known geometric forms [30].

A trifilar pendulum system and electronic stopwatch were used to determine the period of oscillation [18]. The trifilar pendulum was a 6 mm-thick Perspex plate with a weight of 0.98 kg, radius of 210 mm, and radius to the suspension wires of 185 mm. The value of inertia of the plate was theoretically determined to be 0.017 $kg \cdot m^2$. With known geometric forms, the error associated with the experimental technique was 8 percent for a 2.9 kg mass and increased to 15 percent as the mass of the object decreased to 1.4 kg when the CM was coincident with the center of rotation [32]. Offsets between the CM and center of rotation contributed an additional error of between 2.5 and 9.0 percent as the offset ranged from 5 to 20 mm [32].

Geometric Model of Leg and Thigh

Anthropometric data of the leg and thigh segments were determined with the model by Hatze [25]. This model describes the leg segment as an assemblage of elliptical plates. The thigh used elliptical plates to model the segment between the knee and groin and an elliptico-parabolic hoof to describe the thigh segment proximal to the groin level [25].

Linked-Segment Models

A conventional linked-segment model [33] was used to calculate net joint muscle moments for the affected limb of subjects in both samples A and B. This model did not account for the anthropometric changes due to amputation, prosthetic fitting, or footwear and, as such, used BSP of the sound limb to provide normal (nondisabled) input data. Hence, the model should provide comparable estimates to the standard or commercially available linked-segment models that are believed to have been used in previous investigations [14,16–17].

Net joint muscle moments and power were also determined with the customized linked-segment models. Two customized models were necessary, because some prostheses allowed ankle motion and others did not.

Customized Model A was used to describe the kinetic patterns of persons with PFA who were wearing insoles, toe-fillers, and slipper sockets. These devices do not compromise the ankle joint range, because the trimlines remain inferior to the ankle joint. As such, the mass, CM, and *I* of these devices could be combined with the BSP of the remnant foot without affecting the basic assumptions of a conventional linked-segment model [33]. However, to describe the prosthesis or orthosis and shoe within the constraints of the linked-segment model, we had to assume that—

1. The prosthesis or orthosis encompassed only the foot segment, or a portion thereof, and did not restrict ankle motion.

2. The residual foot, prosthesis or orthosis, and shoe could be considered a "lumped" free body segment that rotated about the ankle joint.
3. The lumped segment could be described by a single set of BSP data such that the mass, CM, and *I* of the residual foot, prosthesis or orthosis, and shoe were combined.
4. The location of the CM of the lumped segment could be described relative to the ankle joint and the value of *I* taken through the CM of the lumped free body segment.

Customized Model B was used to describe kinetic parameters of a person wearing a clamshell prosthesis. This type of prosthetic intervention eliminated ankle motion, which was quite convenient for modeling, because the BSP of the leg, residual foot, prosthesis, and shoe could be considered a single lumped free body segment about the knee joint. As such, the mass, CM, and *I* of the prosthesis and shoe need not be partitioned to the foot and leg segment separately to accurately depict the person's lower limb, assuming that the—

1. Clamshell PTB prosthesis eliminated ankle motion or ankle motion could be considered negligible.
2. Clamshell PTB prosthesis encompassed the residual foot and the leg segment or a portion of the leg segment.
3. Residual foot, leg, prosthesis, and shoe could be considered a lumped free body segment that rotated about the knee joint.
4. Lumped segment could be described by a single set of BSP data such that the mass, CM, and *I* of the residual foot, leg, prosthesis, and shoe were combined.
5. Location of the CM of the lumped segment could be described relative to the knee joint and the value of *I* taken through the CM of the lumped free body segment.

These assumptions allowed the anthropometry of the residual foot, leg, and clamshell prosthesis/shoe to be represented as a single free body segment about the knee joint.

These linked-segment inverse dynamics models were coded in MATLAB 5.3 and are available online through the Australasian Digital Theses Program [29].

Gait Equipment

Kinematic data were collected with a six-camera Peak three-dimensional motion analysis system and Motus version 4.3.0 software (Peak Performance Technologies; Centennial, Colorado). This camera setup sampled the location of 20 mm retroflective markers at a rate of 50 Hz. An OR6-5 six-channel strain gauge force platform and an amplifier (Advanced Mechanical Technology, Inc; Waterton, Massachusetts) were used to sample ground reaction force and moment data at a rate of 1,000 Hz, and data were low-pass filtered at the amplifier with a cutoff frequency of 1,050 Hz inherent to the hardware. The Peak-Motus software controlled the synchronization of kinematic and externally measured force data.

Procedures

Assessment

Subjects came to the Queensland University of Technology gait laboratory for a single session during which they were interviewed to obtain a complete medical history. A qualified prosthetist assessed their residuum to determine the amputation level, and where possible, this level was verified through X-ray, surgical reports, or measurement of the residuum length compared with the sound foot [30]. Details about the type of prostheses were noted (**Table 2**). We did not attempt to standardize the footwear of participants—particularly given that many of the prostheses were designed to be included in a particular piece of footwear. A qualified prosthetist evaluated the quality of prosthetic fit and function to ensure that it was adequate.

Determining Body Segment Parameters by Using Plaster Foot Replicas

To obtain the negative mold necessary to produce the plaster foot replicas, we positioned the subjects prone on a treatment plinth with their knee extended and ankle in a neutral angle so the sole of the foot was vertical. Lines horizontally and vertically bisecting the lateral malleolus were marked with indelible pencil before the foot was cast in a non-weight-bearing position with the ankle at 90°. The subjects' feet were cast with plaster of paris bandage and the molds were cut off. The negative molds were filled with dental plaster to the horizontal line bisecting the lateral malleolus. Obvious anomalies in the plaster replica, such as those caused by joins in the plaster bandage, were removed with a surform (rasp) or filled with dental plaster. The casts were then cleaned with sand-screen before being sealed.

Lines to define the increments of immersion were marked on the foot replicas at 1 cm intervals along the negative *z*-axis to approximately 1.5 cm from the sole. Axes were consistent with those illustrated in **Figure 2**. The *x*-axis origin was located at the line vertically bisecting the lateral malleolus. Immersion increments were consecutively marked every 2 cm along the negative and positive *x*-axis from the origin to approximately 2 cm from the heel and from the origin to approximately 4 cm from the toe in the intact foot; these increments were made appropriately shorter for the partial foot.

The volume corresponding to each immersion increment was determined by the volume of liquid displaced and decanted between immersion increments. Foot volume was determined by summation of the volume of each immersion increment. Foot CV was given by the sum of the products of the segment volumes and segment lever arms from the origin of the foot and divided by the total volume of the foot. The segment lever arms were measured with a metal ruler that had increments marked at 1 mm intervals. By determining the density of the plaster replica, we determined estimates of mass and CM.

The values of *I* were obtained for each directional axis of the plaster replicas by orienting the CM of the plaster replica over the center of the trifilar plate and determining the period of oscillation. With knowledge of the physical dimensions of the trifilar pendulum, the mass and CM of the plaster foot, and the period of oscillation, we calculated the values of *I* [18].

Determining Body Segment Parameters by Using Geometric Models of Foot, Leg, and Thigh Segments

Measurements of the respective limb segments were recorded on a measurement form during the subject assessment. These input measurements were later entered into appropriate MATLAB 5.3 routines, and the modeled segment mass, CM, and *I* were stored to file.

Determining Body Segment Parameters Data for Prosthesis and Shoe

The anthropometric characteristics of the prosthesis and shoe were determined by standard techniques describing the dynamics of a rigid body [18]. The mass of the prosthesis and shoe was determined with an electronic scale. The location of the CM of the prosthesis and shoe was given by the intersection of three plumb lines marked on the prostheses when suspended from three different points. With the prosthesis and shoe on the subject, the vertical and horizontal distances from the CM to the proximal joint center were recorded. The value of *I* about each axis was determined with a trifilar pendulum system as described for the plaster foot replicas.

Gait Analysis

Retroflective markers were located on the following anatomical landmarks: the spinous process of the fifth lumbar vertebra, the anterior superior iliac spine, the greater trochanter of the femur, the knee joint space inferior to the lateral epicondyle of the femur, the lateral malleolus, the posterior calcaneus at the level of the fifth metatarsal head marker, and the fifth metatarsal head or its estimated location. Markers were also located midthigh and midleg just anterior to the line connecting the proximal and distal segment markers. The location of the absent fifth metatarsal head was duplicated from the sound foot by placing a ruler posterior to the shod foot and measuring the distance from the ruler to the center of the marker. Markers were located on the outside of the prosthesis or footwear, over the bony landmarks, as necessary.

Participants walked along a level 10 m walkway at their self-selected walking speed. Seven trials were obtained for each lower limb.

Three-dimensional marker coordinates were reconstructed, and any missing data were interpolated with spline routines standard to the Peak-Motus software. Subsequent data processing was undertaken with software written in MATLAB 5.3 [30]. Marker displacement data were filtered with a zero-lag, fourth-order Butterworth digital filter with a 6 Hz cutoff frequency [33]. Individual segment angles relative to the horizontal were determined with an arc tangent function, and joint angles were then determined as the difference between adjacent segment angles [33].

Externally measured force data were filtered with a zero-lag, fourth-order Butterworth digital filter with a 125 Hz cutoff frequency to remove unwanted artifact affecting the signal [30]. Difference in force and moment data from absolute zero were accounted for with use of offsets determined from a 1-second sample of data collected before initial contact. Data were subsampled to match the sampling frequency of the kinematic data, and as such, further filtering was not necessary.

The kinetics of gait were derived for each trial with each of the conventional and customized linked-segment models. Joint powers were calculated as the scalar product of moment and angular velocity and accounted for power transfer across joints [33]. The resultant components of the joint moments and powers were normalized by body mass [34–35].

Individual trials were averaged within each subject for each of the conventional and customized modeling conditions. The magnitude and timing of peak joint moments and powers (**Figures 3** and **4**) were extracted from each subject's ensembled average with a set of computer-mouse-driven crosshairs [30] that traced the moment and power curves and reported the exact value of each data point to

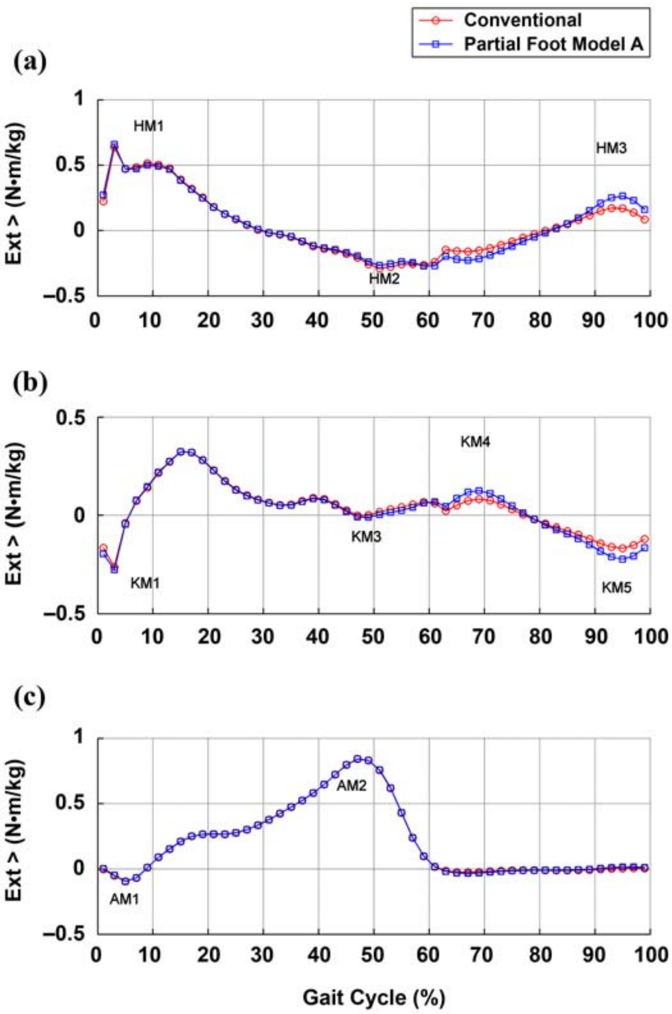

Figure 3.
Average **(a)** hip, **(b)** knee, and **(c)** ankle joint moments for single subject with amputation as calculated with customized partial foot Model A and conventional linked-segment model. Figure illustrates peak joint moments that were analyzed. AM = ankle moment, Ext > = extension moment (positive figures on *y*-axis), HM = hip moment, KM = knee moment.

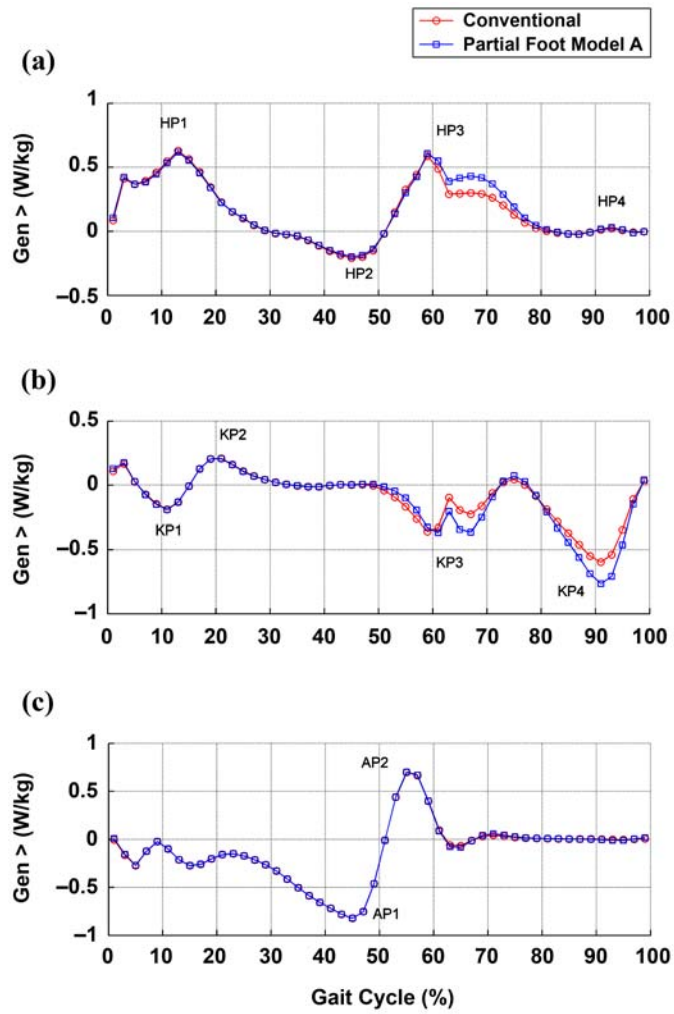

Figure 4.
Average **(a)** hip, **(b)** knee, and **(c)** ankle joint powers for single subject with amputation as calculated with customized partial foot Model A and conventional linked-segment model. Figure illustrates peak joint powers that were analyzed. AP = ankle power, Gen > = power generation (positive figures on *y*-axis), HP = hip power, KP = knee power.

the screen. In this way, the user could identify specific points of interest (**Figures 3** and **4**) in the moment and power curves, such as local maxima or minima, and store these values by clicking the mouse.

Data Analysis

Given the very small sample size, the normality of distribution was tested with the Shapiro-Wilks test, which revealed that some of the BSP data (CM_x [the CM along the *x*-axis from the reference origin] and I_{xx}, I_{yy}, and I_{zz} [the *I* about the *x*-, *y*-, and *z*-axes, respectively, taken through the segment CM]) were not normally distributed ($p < 0.05$). Hence, statistical analysis of the BSP data was approached conservatively, with the strength of the linear relationship between modeled and experimentally derived BSP data determined with the Spearman rank correlation coefficient (ρ). The Shapiro-Wilks test also revealed that the differences between the kinetic data generated by the conventional and customized linked-segment models were not normally distributed for three of the five parameters ($p < 0.05$). Again, a conservative approach was adopted whereby the Wilcoxon signed rank test was used and *p*-values were adjusted for marginal homogeneity. All analysis was undertaken with SPSS version 13 (SPSS, Inc; Chicago, Illinois). Measures of effect size were also determined with a simplified method for calculation of Cohen's *d* [36].

RESULTS

Relationship Between Modeled and Experimentally Derived Body Segment Parameters Data

A strong and significant linear relationship was observed between the modeled and experimentally derived estimates of mass ($\rho = 0.996$, $p < 0.001$), volume ($\rho = 0.999$, $p < 0.001$), CM_x ($\rho = 0.968$, $p < 0.001$), I_{yy} ($\rho = 0.949$, $p < 0.001$), and I_{zz} ($\rho = 0.957$, $p < 0.001$). The relationship between values of CM_z (CM along *z*-axis from reference origin) ($\rho = 0.630$, $p = 0.004$) and I_{xx} ($\rho = 0.601$, $p = 0.008$) were not as strong between the modeled and experimentally derived data yet were significant.

Differences in Anthropometry of Modeled Limb Segments Between Conventional and Customized Linked-Segment Models

Compared with the conventional linked-segment model, the customized model increased the mass of the modeled foot segment, brought the location of the CM closer to the ankle joint, and increased the value of *I* for subjects in Sample A (**Table 3**). Reductions in the mass, CM, and *I* of the residuum compared with the intact foot (conventional foot segment) are detailed in **Table 3**, as is the contribution of the shoe and prosthesis to the overall change in segment anthropometry.

For the person with Chopart amputation in Sample B, amputation reduced the mass of the foot segment, brought the CM closer to the ankle, and reduced the value of *I* compared with the conventional foot segment (**Table 3**). The reduction in the value of mass and change in the inertial characteristics of the leg segment are evident when the mass, CM, and *I* of the customized and conventional leg segments are compared (**Table 3**). The prosthesis and shoe have a substantial mass (1.97 kg), with the location of the CM some 0.35 m inferior to the knee joint, resulting in the value of *I* of the combined prosthesis and shoe being equivalent to a normal leg segment (**Table 3**).

Comparison of Joint Moments and Powers Determined with Conventional and Customized Linked-Segment Models

No differences were observed between the magnitude of the peak joint moments and powers during stance phase or the timing of these during both stance and swing ($p > 0.05$). As such, only the magnitude of the swing-phase moments and powers are reported.

Table 3.
Comparison of segment anthropometry (sagittal plane) between conventional and customized linked-segment model. Conventional foot segment describes mass and inertial characteristics of intact foot and does not account for prosthesis and shoe. Customized foot segment for Sample A includes anthropometry of residuum and prosthesis and shoe, which is combined into single lumped segment. For single subject in Sample B, customized segment described anthropometry of residuum, leg, and clamshell prosthesis and shoe as combined segment about knee joint.

Sample	Mass (kg)	Center of Mass (m)		Inertia (kg·m^2)
		x	***z***	***y***
A: With Ankle Motion				
Conventional Foot Segment	1.055 ± 0.075	0.061 ± 0.003	–0.042 ± 0.005	0.006 ± 0.000
Customized Foot Segment (1 + 2)	1.524 ± 0.203	0.034 ± 0.010	–0.047 ± 0.009	0.008 ± 0.001
1. Residuum	0.792 ± 0.072	0.019 ± 0.009	–0.038 ± 0.002	0.002 ± 0.000
2. Prosthesis and Shoe	0.731 ± 0.261	0.041 ± 0.027	–0.058 ± 0.020	0.006 ± 0.001
B: Without Ankle Motion				
Conventional Foot Segment	1.064	0.054	–0.041	0.0051
Conventional Leg Segment	3.992	0.000	–0.171	0.0533
Customized Segment (1 + 2 + 3)	4.901	0.007	–0.268	0.1548
1. Residuum	0.386	0.011	–0.026	0.0007
2. Leg	2.546	0.000	–0.179	0.0358
3. Prosthesis and Shoe	1.970	0.015	–0.350	0.0608

For the four subjects in Sample A, the customized linked-segment model significantly increased the magnitude of the hip (HM3, $p = 0.03$) and knee (KM5, $p = 0.03$) joint moments during terminal swing by 31 and 25 percent, respectively (**Table 4**). Comparable increases were observed for the peak knee joint power (KP4, $p = 0.046$) during terminal swing, but considerable variability in the peak hip power (HP4) resulted in a nonsignificant difference ($p = 0.26$) despite a large percentage increase (40%) and "medium" effect size ($d = 0.48$), as described in **Table 4**. During initial swing, the change in the knee moment peak (KM4) was "negligible" ($p = 0.15$).

For the subject with Chopart amputation in Sample B, the customized model increased the peak knee and hip joint moments and powers during both initial and terminal swing by between 17 and 39 percent (**Table 4**). No statistical analysis was possible given the single subject in this group.

DISCUSSION

The purpose of this investigation was to understand the degree to which errors in anthropometric input data, caused by partial amputation of the foot and fitting of a prosthesis and shoe, influence the calculation of joint moments and powers so that future investigators would be better informed about the rigor of the anthropometric input data required for a particular research question.

Toward this end, we developed customized geometric models of the partial foot residuum to estimate the mass, CM, and *I* of the intact and partial feet. Linked-segment inverse dynamics models that incorporated these anthropometric descriptions of the residuum, prosthesis, and footwear were also developed.

The geometric model provided estimates of mass, CM, and *I* of intact and partial feet that were strongly related to experimentally derived estimates obtained with incremental immersion and torsional table measurements; thus, we demonstrated the accuracy of the BSP calculated with the geometric model in relation to other well-accepted experimental techniques.

The net joint moments obtained with use of these customized linked-segment models illustrate a systematic increase in the peak knee flexion and hip extension moments during terminal swing phase compared with a conventional model (**Table 4**). Estimates of power generation and absorption at the knee and hip joints reflect differences in the moment profiles observed. These kinetic differences indicate a more accurate portrayal of the activity of the knee flexors and hip extensors to decelerate the knee into full extension and the hip joint into its initial

Table 4.
Comparison of peak swing-phase moments and powers for hip and knee joints derived by using conventional and customized linked-segment inverse dynamic model. See **Figures 3** and **4** for details of exact points examined.

Sample	Inverse Dynamic Model		Difference			
	Conventional	Customized	Absolute	%	*p*-Value	Effect Size (*d*)
A: With Ankle Motion						
Moment						
HM3 (N·m/kg)	0.208 ± 0.042	0.301 ± 0.032	0.093	31	0.03	2.92, huge
KM4 (N·m/kg)	0.116 ± 0.034	0.120 ± 0.034	0.004	3	0.15	0.14, negligible
KM5 (N·m/kg)	–0.193 ± 0.024	–0.256 ± 0.026	–0.063	25	0.03	2.91, huge
Power						
HP4 (W/kg)	0.079 ± 0.080	0.132 ± 0.160	0.053	40	0.26	0.48, medium
KP4 (W/kg)	–0.831 ± 0.176	–1.070 ± 0.280	–0.239	22	0.046	1.18, very large
B: Without Ankle Motion						
Moment						
HM3 (N·m/kg)	0.188	0.242	0.054	22	—	—
KM4 (N·m/kg)	0.040	0.066	0.026	39	—	—
KM5 (N·m/kg)	–0.181	–0.222	–0.041	18	—	—
Power						
HP4 (W/kg)	–0.060	–0.083	–0.023	28	—	—
KP4 (W/kg)	–0.665	–0.797	–0.132	17	—	—

HM = hip moment, HP = hip power, KM = knee moment, KP = knee power.

contact hip flexion angle and to prevent further hip flexion before initial contact. As a point of comparison, the magnitude of these differences were comparable with those observed in the gait of nondisabled subjects changing from a slow-to-normal or normal-to-fast velocity [37–38].

When the customized linked-segment models were used, the differences observed in the swing-phase kinetic data reflect changes in both the mass and mass distribution of the limb segments. For subjects in Sample A, these differences reflect the net increase in the mass and *I* of the customized foot segment given that the shoe and prosthesis are now included as part of the model (**Table 3**). Changes in the value of *I* with the customized foot segment were more modest than might be expected given the increased mass because the location of the CM was much closer to the ankle than it was in the conventional foot segment model (**Table 3**). For the subject in Sample B, the combined foot-prosthesis-shoe dramatically lowered the CM (closer to the ankle), thereby increasing the value of *I* compared with what might be expected from the combination of the conventional foot and leg segments (**Table 3**).

Aside from one investigation [30], previous investigations on the gait of persons with PFA have reported kinetic data for just the stance phase of gait [14,16–17]. The accuracy of these published analyses seem reasonable given that the conventional linked-segment model, which these authors presumably used, is robust to errors in anthropometric input data during stance phase. The only published swing-phase kinetic data [39] used the customized linked-segment model reported here because this investigation stems from the same thesis [30].

Future investigators of PFA gait can now make more informed decisions about the requirement for accurate anthropometric input data in relation to their research questions. For research questions related to the stance phase of gait, conventional linked-segment models that use BSP from persons without limb loss and that do not consider the prosthesis and footwear provide comparable and accurate kinetic data; as such, the additional work necessary to improve the modeled representation seems unnecessary. Should investigators be interested in the kinetics of swing phase, accounting for the unique anthropometry of the residuum and the addition of a prosthesis and footwear within the linked-segment model is recommended to more accurately reflect the eccentric work of the hamstrings and hip extensors during terminal swing phase. The anthropometric and linked-segment inverse dynamic models described in this work provide a means for obtaining these data.

LIMITATIONS

Unfortunately, the generalizability of results is somewhat limited given the small number of subjects recruited. The anthropometry of the subject group lacks the sort of breadth typical of a general population, since most subjects were of similar stature and therefore foot size (**Table 1**). The number of subjects in each subsample of the amputation group is also small (**Table 1**). Future investigators should be mindful of these limitations when generalizing the results of this investigation.

In this investigation, the prosthesis and shoe were considered to be a single segment when the mass and *I* characteristics were measured. As such, retrospectively assessing the relative contribution of the prosthesis or shoe to the kinetic changes observed was not possible. From a practical standpoint, such an assessment matters little, since most prostheses are designed to be worn with a shoe (or indeed a particular shoe). The shortcoming of this approach comes in generalization of the results. For subjects in Sample A, a large proportion of the change in the swing-phase moments and powers is likely attributable to incorporation of just the shoe into the linked-segment model, given that many of the devices (i.e., insoles or carbon-fiber slipper sockets) would not have substantially altered the mass or mass distribution from the shoe alone. This insight may be important for investigators studying even nondisabled gait in shod conditions. The sorts of moment changes reported in this investigation may serve as a reasonable guide in lieu of more accurate assessments given comparison of the anthropometric data in **Table 3** between the conventional and customized models. The differences in the swing-phase kinetics observed for the single subject in Sample B would have been greatly influenced not only by the shoe but also by the clamshell prosthesis, given its substantial mass and distal CM location (near the ankle).

CONCLUSIONS

This investigation determined the accuracy requirements of anthropometric input data for the analysis of the gait of persons with PFA. Toward this end, a geometric model was developed and validated to estimate body segment parameters of various intact and partial feet. The development of conventional and customized linked-segment inverse dynamic models led to the understanding that accurate modeling of the anthropometry of the residuum, prosthesis, and footwear significantly increases the peak joint moments and powers during terminal swing. Investigators that use conventional models that include anthropometric data based on persons without limb loss will underestimate the work of the knee flexors and hip extensors during terminal swing. Estimating stance-phase kinetics with conventional models is accurate, and as such, the work required to generate more accurate models seems unnecessary. Investigators interested in the kinetics of swing phase should account for the unique anthropometry of the residuum and for the addition of a prosthesis and footwear within the linked-segment model to more accurately reflect the eccentric work of the hamstrings and hip extensors during terminal swing.

ACKNOWLEDGMENTS

This work was undertaken as part of a doctoral program at the Queensland University of Technology, Brisbane, Australia, by way of a collaboration between the Centre for Rehabilitation Science and Engineering; School of Mechanical, Manufacturing and Medical Engineering; and School of Mathematical Sciences.

This material was based on work supported, in part, by an Australian Postgraduate Award scholarship.

The authors have declared that no competing interests exist.

REFERENCES

1. De Looze MP, Kingma I, Bussmann JBJ, Toussaint HM. Validation of a dynamic linked segment model to calculate joint moments in lifting. Clin Biomech. 1992;7(3):161–69.
2. Kingma I, Toussaint H, De Looze MP, Van Dieen JH. Segment inertial parameter evaluation in two anthropometric models by application of a dynamic linked segment model. J Biomech. 1996;29(5):693–704. [PMID: 8707800]
3. Cappozzo A, Catani F, Leardini A. Skin movement artifacts in human movement photogrammetry. In: Proceedings of the 14th Congress of the International Society of Biomechanics; 1993 Jul 4–8; Paris, France. p. 238–39.
4. De Looze MP, Bussmann JB, Kingma I, Toussaint HM. Different methods to estimate total power and its components during lifting. J Biomech. 1992;25(9):1089–95. [PMID: 1517270]
5. Cappozzo A, Berme N. Subject specific segment inertial parameter determination—A survey of current methods. In: Berme N, Cappozzo A, editors. Biomechanics of human movement: Applications in rehabilitation, sports and ergonomics. Worthington (OH): Bertec Corp.; 1990. p. 179–85.
6. Davis BL. Uncertainty in calculating joint moments during gait. In: Proceedings of the 8th Meeting of European Society of Biomechanics; 1992 Jun 21–24; Rome, Italy. p. 276.
7. White SS, Lage KJ. Changes in joint moments due to independent changes in cadence and stride length during gait. J Hum Mov Sci. 1993;12(4):461–74.
8. Bach T. A computer simulation of the swing phase in human walking with applications to optimisation of inertial characterists of transfemoral prosthetics limb [dissertation]. [Bundoora, Victoria, Australia]: La Trobe University; 1994.
9. Czerniecki JM, Gitter A, Munro C. Joint moment and muscle power output characteristics of below knee amputations during running: The influence of energy storing prosthetic feet. J Biomech. 1991;24(1):63–75. [PMID: 2026634] Erratum in: J Biomech. 1991;24(3–4):271–72.
10. Miller DI. Resultant lower extremity joint moments in below-knee amputees during running stance. J Biomech. 1987;20(5): 529–41. [PMID: 3611127]
11. Capozzo A, Figura F, Leo T, Marchetti M. Biomechanical evaluation of above-knee prostheses. In: Komi PV, editor. Biomechanics V: Proceedings of the Fifth International Congress of Biomechanics, Jyvaskyla, Finland (International Series on Biomechanics). Baltimore (MD): University Park Press; 1976. p. 366–72.
12. Contini R. Body segment parameters (pathological): Final report. New York (NY): New York University School of Engineering and Science; 1970.
13. Krouskop T, Dougherty D, Yalcinkaya MI, Muilenberg A. Measuring the shape and volume of an above-knee stump. Prosthet Orthot Int. 1988;12(3):136–42. [PMID: 3217243]
14. Mueller MJ, Salsich GB, Bastian AJ. Differences in the gait characteristics of people with diabetes and transmetatarsal amputation compared with age-matched controls. Gait Posture. 1998;7(3):200–206. [PMID: 10200385]
15. Burnfield JM, Boyd LA, Rao SS, Mulroy SJ, Perry J. The effect of partial foot amputation on sound limb loading forces during barefoot walking. Gait Posture. 1998;7:178–79.
16. Boyd LA, Rao SS, Burnfield JM, Mulroy SJ. Forefoot rocker mechanisms in individuals with partial foot amputation. In: Proceedings of the Gait and Clinical Movement Analysis; 1999 Mar 10–13; Dallas, Texas. p. 144.
17. Tang SF, Chen CP, Chen MJ, Chen WP, Leong CP, Chu NK. Transmetatarsal amputation prosthesis with carbon-fiber plate: Enhanced gait function. Am J Phys Med Rehabil. 2004;83(2):124–30. [PMID: 14758298]
18. Maltbaek J. Dynamics in engineering: Classical yet modern, general yet comprehensive, original in approach. Chichester (England): Halsted Press; 1988.

19. Drillis R, Contini R. Body segment parameters. New York City (NY): New York University School of Engineering and Science; 1966.
20. Plagenhoef S, Evans FG, Abdelnour T. Anatomical data for analysing human motion. Res Quart Exerc Sport. 1983; 54:169–78.
21. Fernie GR, Holliday PJ. Volume fluctuations in the residual limbs of lower limb amputees. Arch Phys Med Rehabil. 1982;63(4):162–65. [PMID: 7082139]
22. Drillis R, Contini R, Bluestein M. Body segment parameters: A survey of measurement techniques. Artif Limbs. 1964;25: 44–66. [PMID: 14208177]
23. Contini R. Body segment parameters. II. Artif Limbs. 1972; 16(1):1–19. [PMID: 4648029]
24. McConville JT, Churchill T, Kaleps I, Clauser C, Cuzzi J. Anthropometric relationships of body and body segment moments of inertia. Wright-Patterson Air Force Base (OH): Air Force Aerospace Medical Research Laboratory, Aerospace Medical Division, Air Force Systems Command; 1980.
25. Hatze H. A mathematical model for the computational determination of parameter values of anthropometric segments. J Biomech. 1980;13(10):833–43. [PMID: 7462257]
26. Vaughan CL, Davis BL, O'Connor JC. Dynamics in human gait. Champaign (IL): Human Kinetics Publishers; 1992.
27. Dillon MP, Fatone S, Hodge MC. Biomechanics of ambulation after partial foot amputation: A systematic literature review. J Prosthet Orthot. 2007;19(3 Suppl):2–61.
28. Australian Institute of Health and Welfare [homepage on the Internet]. Canberra (Australia): Australian Government; c1968–2008 [updated 2007; cited 2006 Dec 12]. Interactive national hospital morbidity data (data cubes); [about 2 screens]. Available from: http://www.aihw.gov.au/hospitals/datacubes/index.cfm/.
29. Australasian Digital Theses Program [homepage on the Internet]. Canberra (Australia): Council of Australian University Librarians; c1997–2008 [updated 2001; cited 2007 Nov 2]. Dillon M. Biomechanical models for the analysis of partial foot amputee gait [about 3 screens] Available from: http://adt.library.qut.edu.au/adt-qut/public/adt-QUT20011008.094224/.
30. Dillon MP. Biomechanical models for the analysis of partial foot amputee gait [thesis]. Brisbane (Australia): Queensland University of Technology; 2001.
31. Ackland TR, Henderson PW, Bailey DA. The uniform density assumption: Its effect upon the estimation of body segment inertial parameters. J Appl Biomech. 1988;4(2):146–55.
32. Burkett B. A biomechanical analysis of running for transfemoral amputees [thesis]. Brisbane (Australia): Queensland University of Technology; 1998.
33. Winter DA. Biomechanics and motor control of human movement. 2nd ed. New York (NY): John Wiley & Sons; 1990.
34. Allard P, Lachance R, Aissaoui R, Sadeghi H, Duhaime M. Able-bodied gait in men and women. In: Allard P, Cappozzo A, Lundberg A, Vaughan CL, editors. Three-dimensional analysis of human locomotion. Chichester (England): John Wiley and Sons; 1997. p. 307–34.
35. Craik RL, Dutterer L. Spatial and temporal characteristics of foot fall patterns. In: Craik RL, Oatis CA, editors. Gait analysis: Theory and application. St. Louis (MO): Mosby; 1995. p. 143–52.
36. Thalheimer W, Cook S. How to calculate effect size from published research articles: A simplified methodology [Internet]. Somerville (MA): Work-Learning Research, Inc; 2002. [cited 31 Oct 2007]. Available from: http://work-learning.com/effect_sizes.htm/.
37. Winter DA. Kinematic and kinetic patterns in human gait: Variability and compensating effects. Hum Mov Sci. 1984; 3:51–76.
38. Winter DA. Biomechanical motor patterns in normal walking. J Mot Behav. 1983;15(4):302–30. [PMID: 15151864]
39. Dillon MP, Barker TM. Preservation of residual foot length in partial foot amputation: A biomechanical analysis. Foot Ankle Int. 2006;27(2):110–16. [PMID: 16487463]

Submitted for publication November 18, 2007. Accepted in revised form June 10, 2008.